AFGL-TR-78-0129

LEVEL II

ADA084241

Correlation of Radar and Satellite Date to Determine Birkeland Current Signatures

Robert J. Spiger

Geophysics Program AK-50
University of Washington
Seattle, Washington

April 1978

Final
31 October 1976 - 31 December 1977

Approved for public release; distribution unlimited

AIR FORCE GEOPHYSICS LABORATORY
AIR FORCE SYSTEMS COMMAND
UNITED STATES AIR FORCE
HANSCOM AFB, MASSACHUSETTS 01731

Unclassified

SECURITY CLASSIFICATION OF THIS PAGE (When Data Entered)

(19) REPORT DOCUMENTATION PAGE

READ INSTRUCTIONS BEFORE COMPLETING FORM

1. REPORT NUMBER (18) AFGL TR-78-0129	2. GOVT ACCESSION NO. AD-A084 241
3. RECIPIENT'S CATALOG NUMBER	
4. TITLE (and Subtitle) (6) CORRELATION OF RADAR AND SATELLITE DATA TO DETERMINE BIRKELAND CURRENT SIGNATURES	5. TYPE OF REPORT & PERIOD COVERED (9) Final [redacted]c Report, 31 Oct [redacted]76 — 31 Dec [redacted]77
	6. PERFORMING ORG. REPORT NUMBER
7. AUTHOR(s) (10) Robert J. Spiger	8. CONTRACT OR GRANT NUMBER(s) (15) F19628-77-C-0042
9. PERFORMING ORGANIZATION NAME AND ADDRESS Geophysics Program AK-50, University of Washington, Seattle, Washington 98195	10. PROGRAM ELEMENT, PROJECT, TASK AREA & WORK UNIT NUMBERS 35160F (16) 2311G202 (17) G2
11. CONTROLLING OFFICE NAME AND ADDRESS Air Force Geophysics Laboratory, Hanscom AFB, Massachusetts, Monitor/Michael Smiddy/PHP	12. REPORT DATE (11) Apr[redacted] [redacted]78
	13. NUMBER OF PAGES 27
14. MONITORING AGENCY NAME & ADDRESS (if different from Controlling Office) (12) 27	15. SECURITY CLASS. (of this report) Unclassified
	15a. DECLASSIFICATION/DOWNGRADING SCHEDULE

16. DISTRIBUTION STATEMENT (of this Report)

Approved for public release; distribution unlimited

17. DISTRIBUTION STATEMENT (of the abstract entered in Block 20, if different from Report)

18. SUPPLEMENTARY NOTES

19. KEY WORDS (Continue on reverse side if necessary and identify by block number)

Birkeland Currents, Particle Precipitation, Backscatter Radar.

20. ABSTRACT (Continue on reverse side if necessary and identify by block number)

A set of techniques has been developed for analyzing the particle and magnetometer data from the S3-2 satellite in conjunction with data from the Chatanika radar with the objective of determining radar signatures of Birkeland currents. Computer programs have been completed and tested for handling particle data pitch angle distributions. Limited available joint data from both satellite and radar has indicated a broad sheet current structure with a maximum field perturbation of ~ 75γ extending over 5.4° of geomagnetic (over) degrees

(approximately 75 gamma

DD FORM 1 JAN 73 1473 EDITION OF 1 NOV 65 IS OBSOLETE

S/N 0102-LF-014-6601

Unclassified

SECURITY CLASSIFICATION OF THIS PAGE (When Data Entered)

370 570

(Cont)

20. latitude for orbit 1144. Radar observations indicate a diffuse aurora over the same geomagnetic region. Based on this data and previous sounding rocket data, a tentative conclusion indicates that Birkeland current structures may be present for most stable auroral configurations.

A

Availability Codes

Avail and/or
special

A

INTRODUCTION

Auroral zone electron precipitation varies over several orders of magnitude depending on auroral activity. The most obvious visual evidence of this precipitation is the auroral arc. A typical arc is caused by precipitating electrons in the 1-10keV range producing light emission in the upper atmosphere. Ionization associated with these emissions is detectable using ground based radar equipment such as the Chatanika incoherent back-scatter radar. As the electrons producing an arc precipitate, they often form a sheet current directed out of the atmosphere. These currents and the associated return currents have been termed Birkeland currents. Measurements by a number of investigators using both sounding rockets (Park and Cloutier, 1971, Casserly and Cloutier, 1975) and satellites (Zmuda and Armstrong, 1974) have shown the current sheets to be common features associated with auroral activity. Monitoring of Birkeland current sheets requires flight magnetometers of high sensitivity and a considerable amount of analysis of the flight data. The purpose of this work has been to correlate the data from the S3-2 satellite, launched in late 1975, with simultaneous data available from the Chatanika radar site in order to determine if radar observations could provide ground-based signatures of Birkeland current systems.

Park, R. J. and P. A. Cloutier, Rocket-based measurement of Birkeland currents related to an auroral arc and electrojet, J. Geophys. Res.,76, 7714, 1971.

Casserly, R. T. and P. A. Cloutier, Rocket-based magnetic observations of auroral Birkeland currents in association with a structural auroral arc, J. Geophys. Res.,80, 2165, 1975.

Zmuda, A. J. and J. C. Armstrong, Flow pattern of field-aligned currents, J. Geophys. Res., 79, 4611, 1974.

The remainder of this report is divided into several sections. These sections present a description of some of the previously determined Birkeland current characteristics and the approach designed to compare the satellite data with the radar data. Next, the available data are described and the analysis techniques are applied. In the final section, results are discussed based on the satellite and radar data and on previous information derived from sounding rocket measurements. Conclusions with regard to the data and recommendations for further data comparisons are made. An appendix at the end of the report outlines and lists the computer codes developed for use with the data.

Method

The presence of Birkeland currents has typically been inferred from measurements by flight magnetometers on polar orbiting satellites or sounding rockets. Sheet currents associated with an auroral arc tend to extend in a magnetic east-west direction, often for hundreds of kilometers. Thus, to a first approximation, the sheet currents may be regarded as infinite and the variation of the magnetic field due to these currents lies in a magnetic east-west direction for currents directed into or out of the ionosphere. For a magnetometer passing through such a sheet current the change in the east-west component of the magnetic field (B_x) is related to the magnitude of the current by the relation:

(1) $|\Delta\bar{B}_x| = |\bar{j}_z|\ \Delta w\ \mu_0$ where $\bar{j}_z$ is the sheet

current density in amps/m^2, and Δw is the magnetic north-south extent of the current sheet in meters. For a typical Birkeland current system consisting of an upward and a downward current sheet (in the z direction) in close proximity, a flight magnetometer would show a perturbation in B_x such as that in Figure 1. By measuring the magnitude of the perturbation in B_x and the spatial distance over which it occurs, the magnitude and location of the current densities can be inferred. Typical current densities are on the order of 10^{-6} - 10^{-5} amps/m^2 for a bright arc. These densities produce perturbations in B_x on the order of 10 - 100γ. Given an ambient field on the order of $4 \cdot 10^4\gamma$ the task of extracting a small perturbation can be quite difficult, particularly if there are other perturbations caused by stray magnetic fields or non-inertial motions of the spacecraft. Nonetheless, the magnetometer does provide the best method for the measurement of Birkeland current systems.

For an auroral arc with an energy spectrum which peaks in the 1-20 keV range, measurements have indicated that a significant fraction of the upward Birkeland sheet current is carried by the incident energetic electrons (Spiger and Anderson, 1975). It is inferred that the remainder of the upward current and the return downward current are carried by electrons below the energy range measured (<0.5 keV). Measurements by other observers also indicate a similar current pattern (Arnoldy, 1974). Thus, for an auroral arc, the measurement of energetic particle fluxes is also an indication of a Birkeland current system. It should be noted

Spiger, R. J. and H. R. Anderson, Electron currents associated with an auroral band, J. Geophys. Res. 80, 2161, 1975

Arnoldy, R. L., Auroral particle precipitation and Birkeland currents, Rev. Geophys. and Space Phys. 12, 217-231, 1974

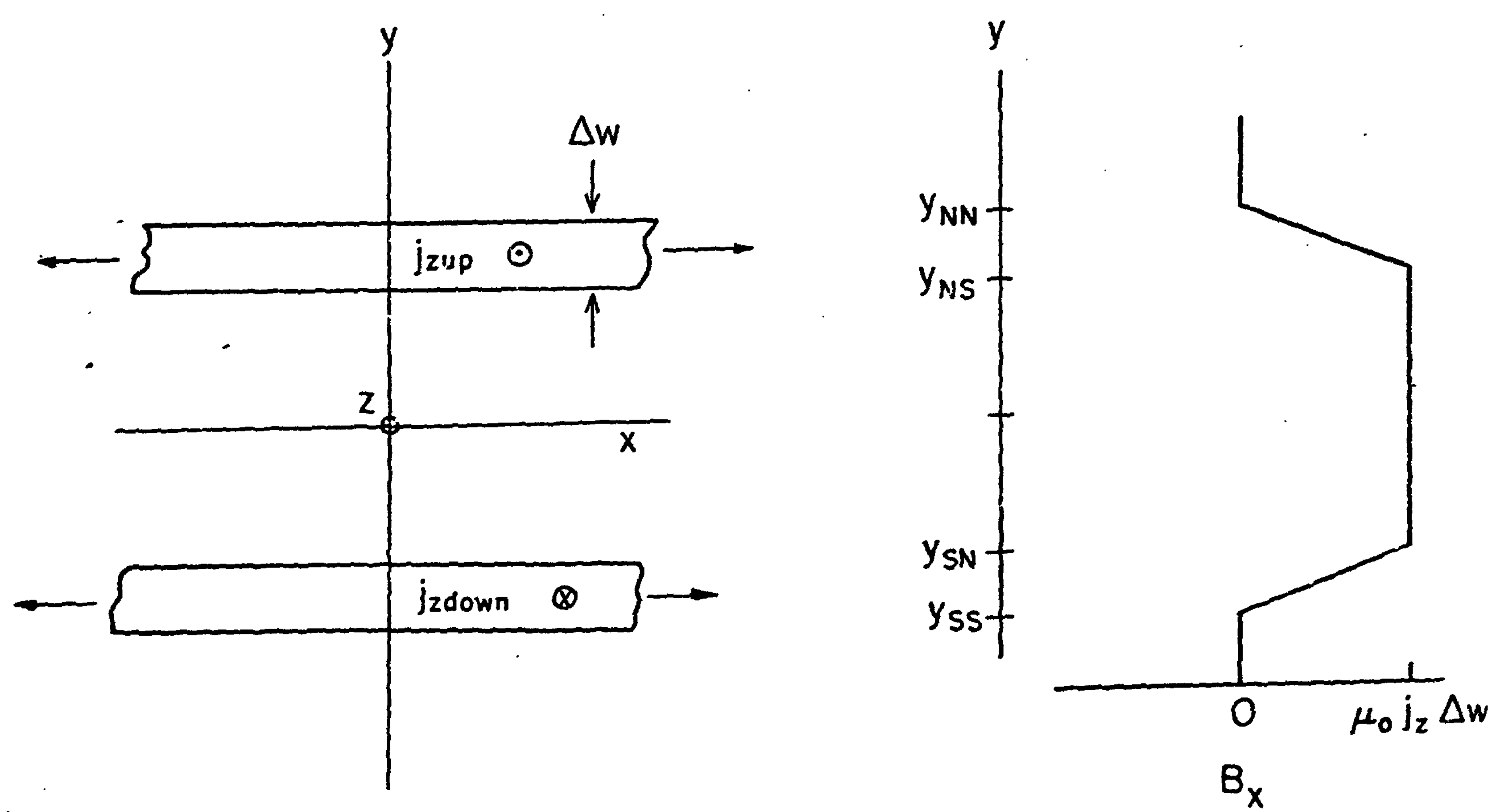

Figure 1: Perturbation induced in the x component of the magnetic field by two finite thickness sheet currents of density j_z and width Δw.

however, that the statistics on this type of measurement are not high enough to relate the magnitude of the sheet current density to the electron flux at any particular energy.

One of the principal parameters measured by the incoherent backscatter radar at Chatanika is the electron density produced by the ionizing effect of incident energetic electrons. By measuring ionization as a function of range and elevation, a grid of electron density values can be constructed as a function of latitude, longitude and altitude. Once the electron density is known as a function of these parameters, the incident energy spectrum may be inferred using a technique analagous to the deconvolution of multiple energy gamma ray spectra in a scintillation crystal. This technique is described more fully in the paper by Vondrak and Barron, 1977. The approach originally designed to correlate the S3-2 data with the radar data was as follows:

a) Magnetometer data on the spacecraft would be used to measure Birkeland current sheets.

b) Simultaneous radar coverage would provide electron density profiles and hence information on the incident energy spectrum.

c) By using the electrostatic analyzer on the spacecraft, the incident electron spectrum would be measured for comparison with that derived from the electron density radar data.

d) Through the observation of a large number of passes over the auroral zone a statistical base can be built up relating the current sheet measurements to the measured particle spectra and the radar electron density data. These comparisons can then be used to determine:

Vondrak, R. R. and M. J. Barron, Radar measurements of the latitudinal variation of auroral ionization, Radio Science II, 939, 1976.

(i) whether the measured particle spectrum agrees with that inferred from the radar data.

(ii) how the measured particle spectrum correlates with the measured sheet current density.

(iii) whether an unambiguous relation then exists between the Birkeland current configuration and the electron density profiles measured by the radar.

Data

A survey of the available data disclosed only two orbital passes near the Chatanika radar during which both the radar and the appropriate satellite instruments were operating. These were orbits 1130 and 1144 of the S3-2 spacecraft. The original preparation for data handling had assumed that a considerably larger number of orbits would be available for analysis and computer codes were devised to handle the magnetic tapes of particle data. Lacking the reduced particle data until late in the program, the computer codes were tested using tapes of sounding rocket data and were found to perform satisfactorily (see Appendix A). Because of the relatively small amount of data actually available, the two orbits were inspected using the computer printouts supplied by AFGL.

Orbit 1130

During orbit 1130 the S3-2 satellite passed approximately 11^{o} in longitude west of Chatanika. Auroral activity for this orbit was very low with the K_p indices for this date (February 24, 1976), being

$K_p = 0^+$ to 1. Passage of the satellite through the region from 65^0 N. Lat. to 68^0 N. Lat. occurred between times 8:23 and 8:25 UT. During this time the magnetometer data supplied by B. Shuman show no evidence of perturbations indicating a Birkeland current configuration. Radar electron density measurements made during this time period by R. Vondrak (private communication) show electron density values of $<10^4$ el./cm^3 at all points. These levels are not significantly different from noise. A survey of the electrostatic analyzer data shows no significant particle precipitation during this passage over the Chatanika region. All sky camera data from the University of Alaska show no auroral activity either in the Chatanika area or farther north at Ft. Yukon. A survey of DMSP images revealed no coverage for this region during this time period.

Orbit 1144

During orbit 1144 the satellite passed approximately 10^0 in longitude west of Chatanika. Auroral conditions for this orbit were slightly more active than for orbit 1130 with K_p indices for this date (February 25, 1976) ranging from 0^+ to 2^-. Figure 2 shows the ground track of the satellite relative to the radar observation site at Chatanika. Magnetometer records from Ft. Yukon indicate very little magnetic activity during the time period 0816 - 0820 UT when the satellite was passing. A slight deflection in the Ft. Yukon D axis magnetometer of $\sim 25\gamma$ occurs during the time period from 0745 - 0830. All sky camera records from Poker Flats and Ft. Yukon show no auroral activity until after 1000 UT when bright aurorae were noted at Poker Flats. Records show no DMSP images over the region at this time.

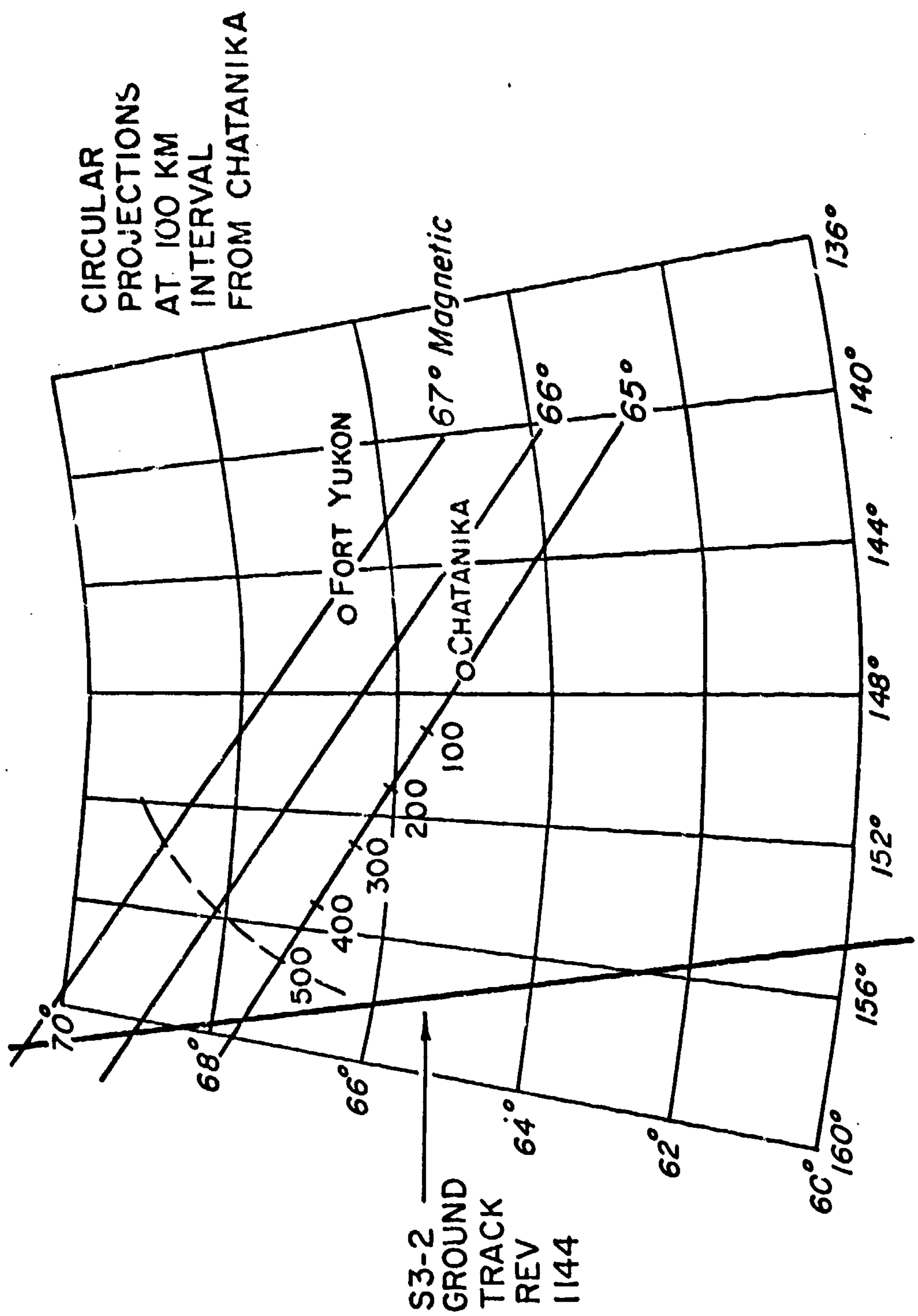

Figure 2: Ground track of S3-2 satellite for orbit 1144

The flight magnetometer data supplied by B. Shuman shows a slight deflection in the east-west component of the magnetic field during the time period 08:17:27 to 08:19:41. This deflection is shown in Figure 3. The variation in this component of the field is quite gradual indicating a broad pair of sheet currents with the downward sheet current lying equatorward of the upward sheet current. The maximum amplitude of the variation in B_x is $\sim 75\pm25\gamma$. This general configuration would indicate that the two sheet currents are adjacent and relatively constant in current density over the magnetic north-south extent of the system (65.2^0 - 70.6^0). For a broad current system such as this, the relation $\Delta B_x = \Delta w|j_z|$ yields an approximate value of current density given by:

$$\Delta B_x = 75\gamma = 3.25 \cdot 10^5 \mid j_z \mid \mu_o$$

$$j_z = 1.81 \cdot 10^{-7} \text{ amp/m}^2$$

where the sheet current width Δw is taken as $\sim$ 325km = $3.25 \cdot 10^5$m.

This is a relatively low value of current density as might be expected from such a spatially diffused current system.

Particle data for orbit 1144 were supplied by R. Vancour. Since the orbit passes to the west of Chatanika, we have assumed that what auroral activity is present will be aligned in a magnetic east-west direction, and thus we have correlated the radar, particle and magnetic observations according to magnetic latitude. In the region of the downward sheet current, the indicated energetic particle flux is very low. A pitch angle scan from 08:17:41 - 08:17:51 shows only one count in one channel implying fluxes $< 4 \cdot 10^{-7}$ part./cm^2 sr-keV-sec at 16.9 keV. This distribution was taken near 66^0 magnetic latitude.

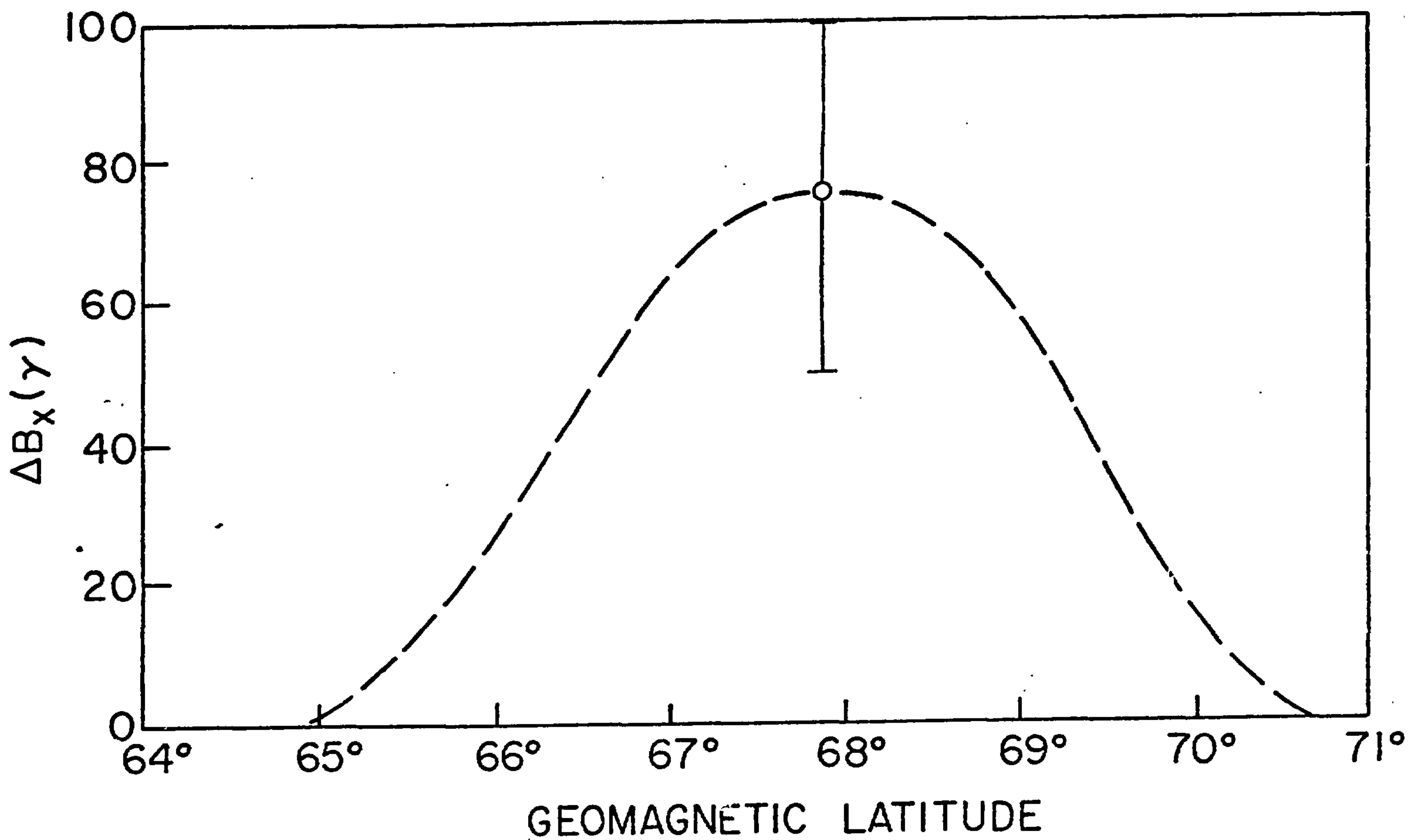

Figure 3: East-west component of the magnetic field as measured by the S3-2 flight magnetometer.

Above 67^0 magnetic latitude, the energetic electron flux increases and tends to be greater in the forward hemisphere. A pitch angle distribution from 08:18:38 - 08:18:48 UT is shown in Figure 4. This scan occurs at $\sim 68.5^0$ magnetic latitude. Flux is averaged over 1-6 keV which represents roughly the peak in the energy spectrum for this scan. Average fluxes range from 10^7 part./cm^2 sec sr keV at forward angles to $<10^6$ part./cm^2 sec sr keV at the backward angles. If we use this pitch angle distribution to calculate an average current density j_x due to the energetic particles, we obtain a value of $j_z = 2\Pi e\int_0^{\Pi} J(\alpha) \cos\alpha \sin\alpha d\alpha \; \Delta E = 1.1 \cdot 10^{-7}$ amp/m^2 where $J(\alpha)$ is the flux, α is the pitch angle and ΔE is the energy interval covered by the average flux. Note the comparison between this value and the value of $1.85 \cdot 10^{-7}$ amp/m^2 derived from the magnetometer data.

The incident energy spectrum for this pitch angle scan is shown in Figure 5. It can be seen that a relative peak in the flux occurs near 3.3 keV with another increase at low energy. The statistical variations are shown by the error bars and are large due to the low fluxes. This energy spectrum was averaged over pitch angles 0^0 - 90^0.

The radar data for orbit 1144 were supplied by R. Vondrak. An elevation scan was taken looking in a magnetic north direction from Chatanika. The time span covered by the scan was 8:16:02 to 8:24:49 UT. From the raw data a plot of electron density was made as a function of range and altitude. Figure 6 shows the derived contour plot. The radar indicates a quiet diffuse aurora north of Chatanika. The radar measurements also allow the calculation of the horizontal currents associated with the

R. R. Vondrak, private communication, 1978.

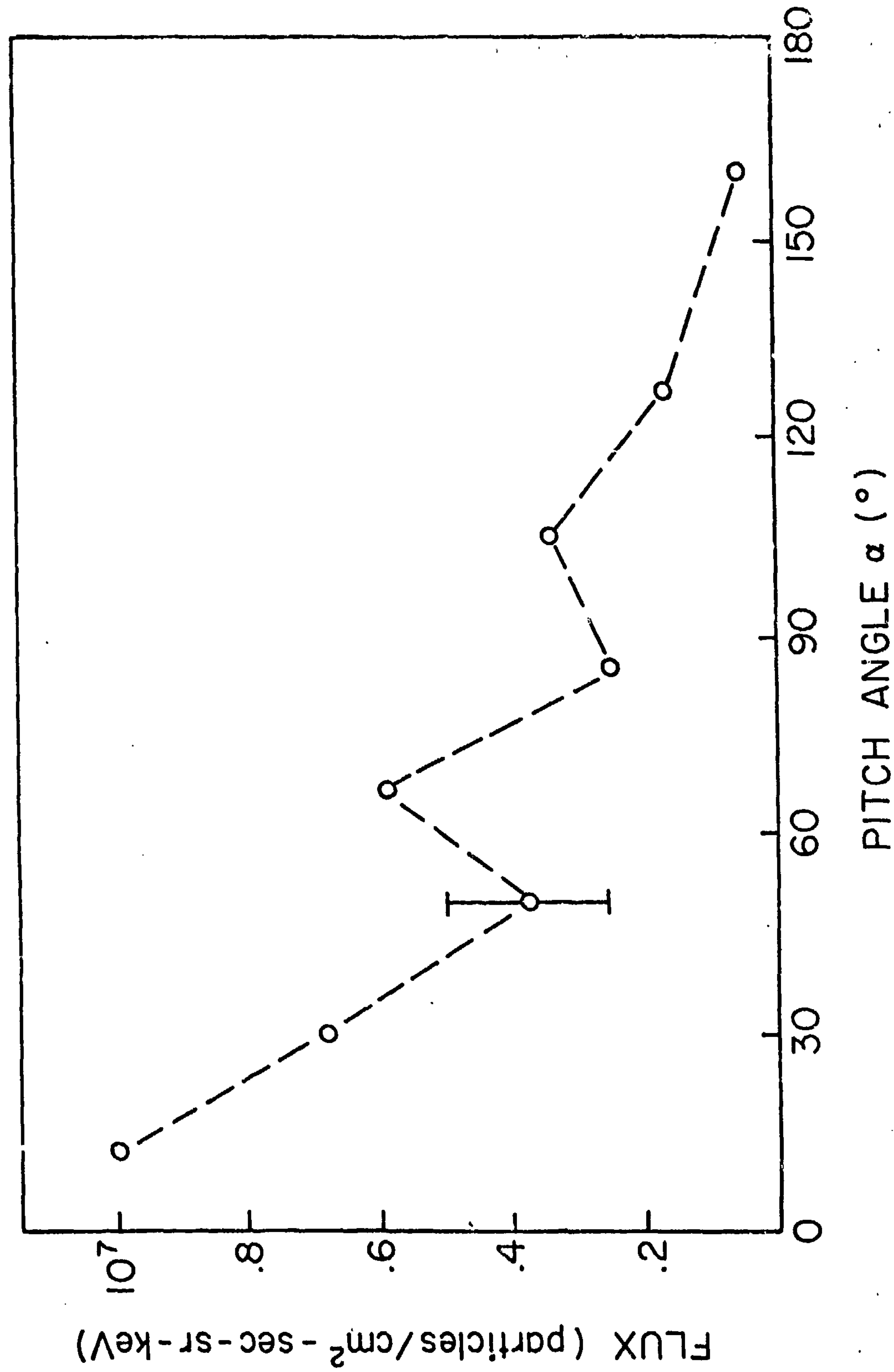

Figure 4: Pitch angle distribution of electron flux averaged over the range 1-6 keV.

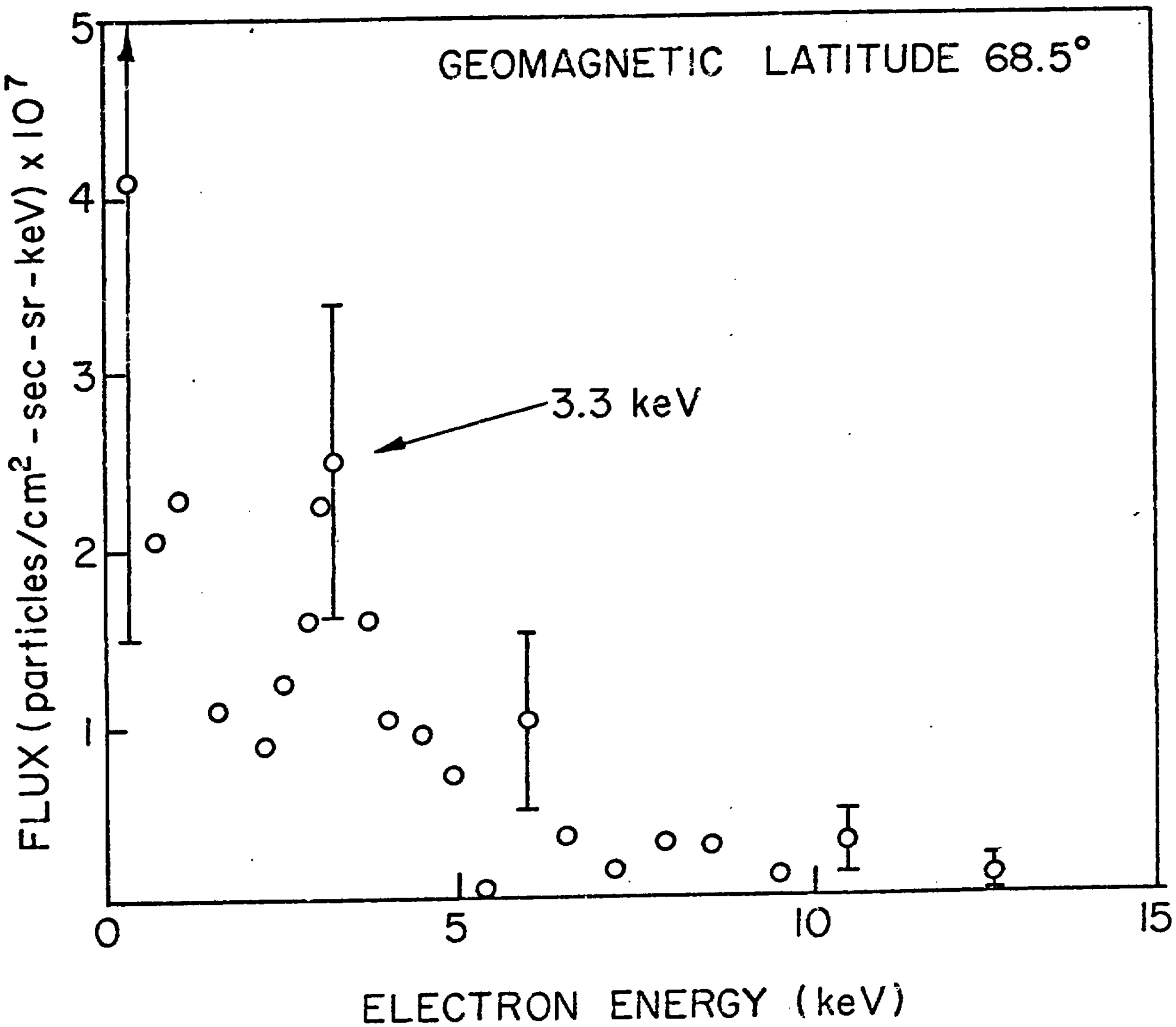

Figure 5: Electron energy spectrum averaged over pitch angles 0^{o} - 90^{o}.

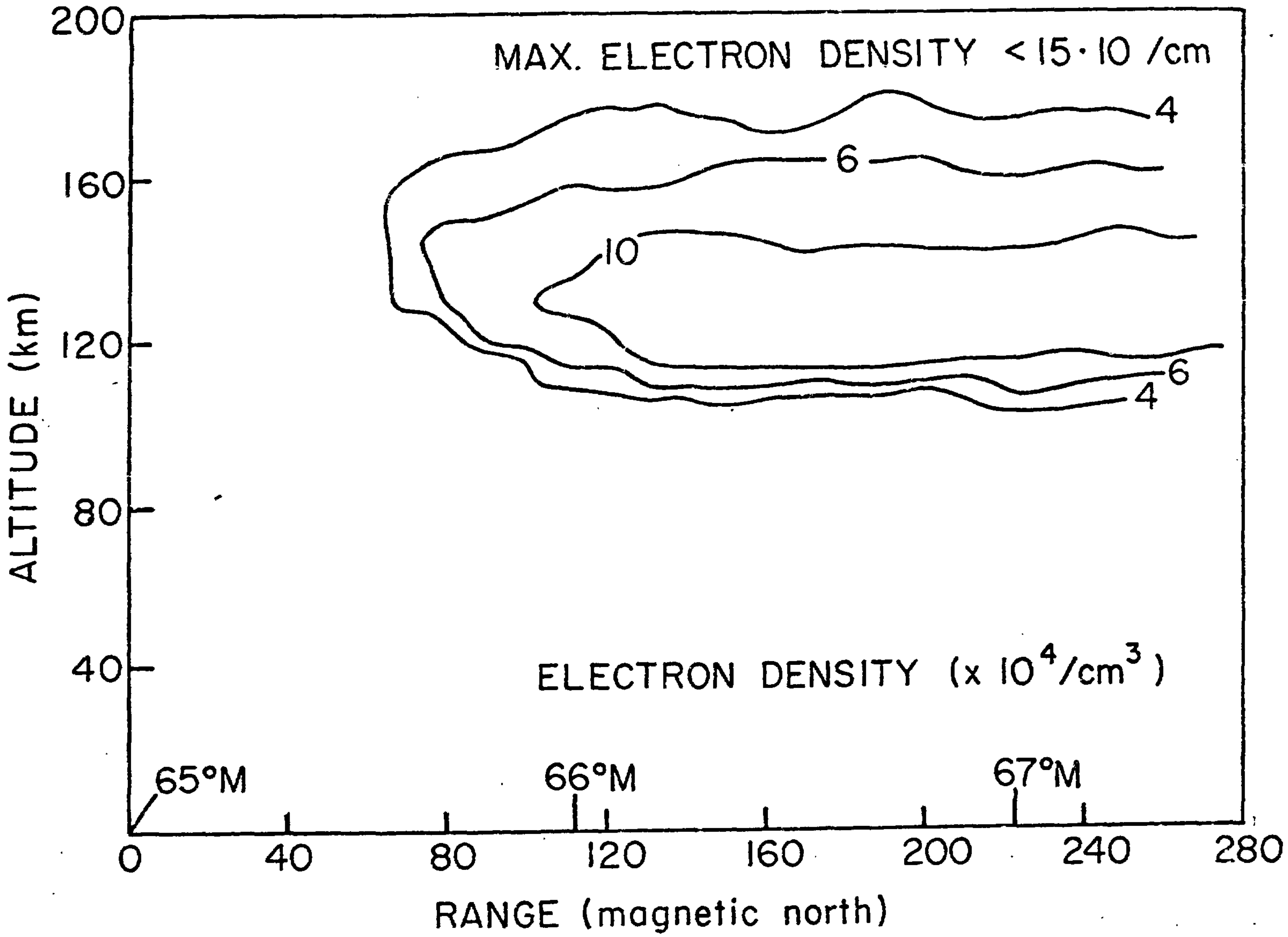

Figure 6: Contour plot of electron density vs range and altitude as measured by Chatanika radar.

electron precipitation. Figure 7 shows the calculated easterly and northerly currents based on the radar data. Note the gradient in current near 80 km north of Chatanika. This gradient implies a field-aligned current estimated to produce an $\sim$ 100γ variation in B_x at satellite altitude (R. Vondrak, 1978). The region of significant flux from the particle detectors lies north of the range of the radar for this set of auroral conditions, thus making a close comparison between radar and particle data difficult.

DISCUSSION

While the limited data prevents a statistically significant correlation between the satellite and radar data, we feel that a number of results of this work can be pointed out and some tentative conclusions drawn. The magnetometer data indicates a broad current sheet configuration in which the downward current lies equatorward of the upward current. The upward current is partially carried by the energetic electrons in the 1-6 keV range. No evidence is seen for the presence of energetic electrons as major current carriers in the southern current sheet. A similar result has been noted in experiments on bright auroral arcs tens of kilometers wide using sounding rockets (Casserly and Cloutier, 1975). Fluxes in these two types of events vary by almost two orders of magnitude, yet the general configuration and makeup of the current sheets appear quite similar. These two results may indicate that the southern downward return

Casserly, R. J. and P. A. Cloutier, etc. See C.

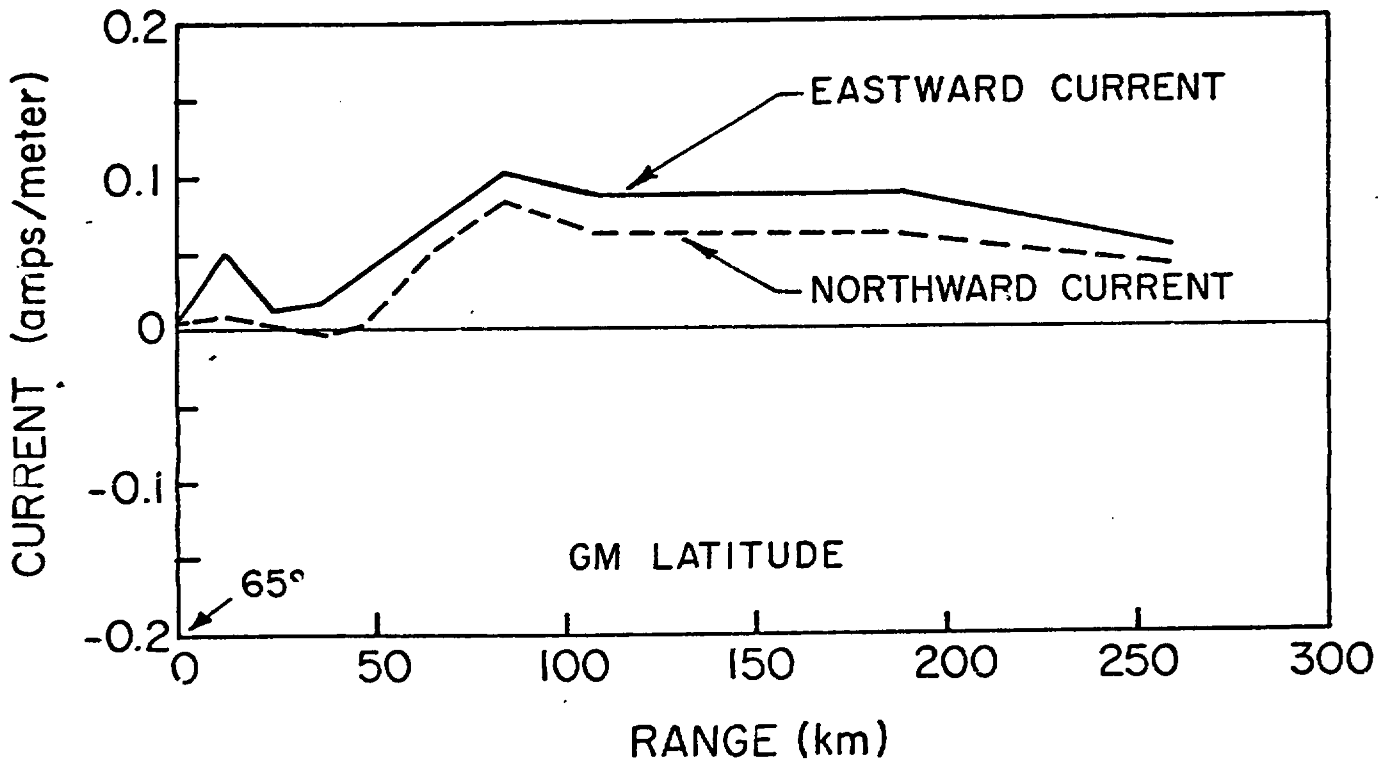

Figure 7: Horizontal currents associated with the diffuse aurora as measured by Chatanika radar. Range is in a magnetic north direction from Chatanika.

current is generally carried by low energy particles and that a significant fraction of the upward northern current is carried by the energetic electrons.

Use of the radar derived currents estimates a variation in B_x of $\sim 100\gamma$ at satellite altitude. This compares with a measured value by the flight magnetometer of $\sim 75 \pm 25\gamma$. The values are similar although the center of the geomagnetic latitude of the current sheets as measured by the satellite (65.2^{0} - 70.6^{0}) lies well north of the position of the gradient in the horizontal current as measured by the radar (~ 65.7). Lacking all-sky camera data, it is not certain that auroral forms will be constant through the 10^{0} in longitude that we extrapolate over or that alignment will coincide exactly along a magnetic east-west direction. Thus the variation in position of the maximum variation in B_x should perhaps not be taken too seriously.

Use of the radar data to calculate the incident electron spectrum shows a similar position for the calculated peak in the energy spectrum. The furthest position north for the radar-derived spectrum is $\sim 67.2°$ geomagnetic latitude. This position is near the southern edge of the northern current sheet as measured by the satellite. The fluxes are higher by an order of magnitude than those measured by the satellite, which may indicate an auroral arc forming farther south to the east of the satellite position and within the radar range.

Based on the satellite observations and the sounding rocket observations, it appears that the formation of Birkeland current systems is the normal situation for stable auroral conditions in the evening sector. Apparently, a large localized electrojet is not a required condition for field-aligned current systems. If so, then one can assume that a radar indication of particle precipitation from diffuse auroral conditions to bright arcs also indicates the presence of a Birkeland current system.

Although the low fluxes and small field perturbation limits the accuracy of the result, it is interesting to note the general agreement between current densities derived from the magnetometer and particle data. Data from the satellite particle detector extends to a lower energy than the previous measurements made by sounding rocket (Spiger and Anderson, 1978), and it would be interesting to see if the lower energy channels would indicate a significant return current in more active auroral conditions.

The current work and previously mentioned sounding rocket experiments both deal with relatively stable conditions in the evening sector. During breakup the analysis of current models becomes much more difficult, although sounding rocket data indicates that a relatively simple current structure may persist in breakup conditions (Anderson, 1978). Stable situations tend to occur again during early morning hours. An interesting problem is whether the relative location of the upward and return current sheets changes in the morning sector in conjunction with electrojet reversal.

Based on the data available data, the following tentative conclusions are drawn. Because of the low statistical base, these conclusions should be considered subject to further verification.

(1) The formation of Birkeland current systems appears to occur over a wide range of auroral conditions in the evening sector ranging from subvisual to IBC II activity. Energetic electrons

Anderson, H. R., private communication, 1978.

are major current carriers in the northern upward sheet and lower energy particles carry the majority of the current in the southern downward sheet.

(2) The spatial relations and current carriers for the current sheets appear to be similar over the same wide range of conditions although the spatial scale varies greatly.

(3) Radar indication of a stable evening auroral precipitation pattern may be a valid indication of the formation of a Birkeland current system.

A number of suggestions for further data comparisons of interest can be made as a result of this work. Some of these are indicated below.

(1) Compare magnetometer, particle data, and radar data (if possible) over a more continuous range of conditions to determine if the above conclusions generally apply. Try to select orbits passing nearer Chatanika and with greater auroral activity.

(2) Make similar comparisons in the morning sector, particularly after electroject reversal to investigate whether the current configuration changes.

(3) Look at the particle and magnetometer data during more active conditions for evidence of electrons at the low end of the particular detector energy range as current carriers for the downward return current.

The techniques developed to analyze this data show reasonable agreement between particle detector and magnetometer results and would be applicable to further investigations as outlined in the suggestions above.

APPENDIX A

The principal computer program developed for this project was designed to accomplish several tasks:

1) Extract the particle flux data from magnetic tape and sort it with respect to time, pitch angle and energy.
2) Select individual scans in pitch angle for further analysis.
3) Calculate the precipitated energy and/or incident electron current produced by the incident flux.

Actual data from the satellite was received late in the project. As a result the program was tested using an electron data tape from a sounding rocket experiment. All aspects of the program were found to work satisfactorily. An inspection of the satellite data available showed a very limited particle flux for the two available orbits. In addition, spurious counts during half of the pitch angle scans complicate the handling of the data. Given these considerations, it was deemed simpler to process the particle data by hand using the computer printouts than to obtain and process the actual reduced data tapes. A listing of the computer program SISCAN is provided on the following pages. The program is written in FORTRAN IV for the University of Washington CDC 6400 computer and should be usable on any comparable facility with minor revisions of input and output statements. The parameters EPASS (I) are the energy passbands of the detector. The parameter ACODE gives the maximum pitch angle to which the calculations will be made. This allows the precipitated energy or the current to be calculated for pitch angles forward of any given value. The energy precipitated in each band is given by ESM(I) in ergs/cm^2.

```
      PROGRAM SISCAN(INPUT.OUTPUT,PUNCH,TAPE1,TAPE2=PUNCH)
      DIMENSION A(9,1000),SS(9,25),DTH(25),EPASS(9)
      DIMENSION ARRAY(512)
      DIMENSION SUM(9),ESUM(9)
      DIMENSION  T(11),  D(11,48)
      DIMENSION SC(9,25),DT(25),SM(9),ESM(9)
      ACODE = 30.
      EPASS(1)= 10.
      EPASS(2)= 10.
      EPASS(3)= 186.528*10.**(-9.)
      EPASS(4)=30.975   *10.**(-9.)
      EPASS(5)=23.04    *10.**(-9.)
      EPASS(6)=18.312   *10.**(-9.)
      EPASS(7)=10.92    *10.**(-9.)
      EPASS(8)=2.94     *10.**(-9.)
      EPASS(9)=1.064    *10.**(-9.)
      IER = 0
      DO 10 I=1.  905
      CALLREADBLK(1,1,512,ARRAY,IRETURN)
      IF (I.LE. 810)10,37
   37 CONTINUE
      DO 12 L=1,11
      T(L) = ARRAY(49*(L-1) +1)
      IF (L.EQ.11)12,14
   14 DO 13 N=1,48
      D(L,N)= ARRAY(49*(L-1) + N+1)
   13 CONTINUE
      IF (D(L,24).LE.0.1) GO TO 21
      IX= 10*(I- 811)+L-IER
      A(1,IX)= T(L)
      A(2,IX)= D(L,24)
      A(3,IX)= D(L,22)
      A(4,IX)= D(L,25)
      A(5,IX)= D(L,28)
      A(6,IX)= D(L,31)
      A(7,IX)= D(L,34)
      A(8,IX)= D(L,37)
      A(9,IX)= D(L,40)
      GO TO 12
   21 IER = IER +1
      PRINT 56, IER
   56 FORMAT(I6)
   12 CONTINUE
   10 CONTINUE
   47 FORMAT(9E9.2,17)
      DO 15 NX=1,40
   15 PRINT 47,(A(NO,NX),NO=1,9),IER
      MP=0
      DO 315 MO=1,25
      MS = MO+MP
      IF(A(2,MS+2).GE.A(2,MS+1).AND.A(2,MS+1).LE.A(2,MS))GO TO 449
  315 CONTINUE
  449 INT = 0
  450 DO  451 NI=1,25
      DO 452 NJ=1,9
```

```
452 SS(NJ,NI)= A(NJ,MS+NI+1+INT)
    PRINT  55, (SS(IY,NI), IY =1,9)
    IF(NI.EQ.1)GO TO 451
    IF(SS(2,NI).LE.SS(2,NI-1))453,451
 55 FORMAT(9E10.2)
453 MOP  = NI-1
    INT = INT + NI    -1
    GO TO  460
451 CONTINUE
460 DTH(1) = SS(2,1)
    DO 461 NK=2,MOP
    DTH(NK) = SS(2,NK)-SS(2,NK-1)
461 CONTINUE
    DO  464 NN=3,9
    SUM(NN)= 0.0
    MOQ =MOP-1
    DO 462 NM = 1,MOQ
    IF (NM.EQ.1)GO TO 802
   0IF(NM.GT.1.AND.SS(2,NM).GT. ACODE.AND.SS(2,NM-1).GE.ACODE)SS
   (NN,NM-1)=0.0
    IF(NM.GT.1.AND.SS(2,NM).GE. ACODE.AND.SS(2,NM-1).LT.ACODE)801,802
8010SS(NN,NM) =SS(NN,NM-1)+(ACODE-SS(2,NM-1))*(SS(NN,NM)-SS(NN,NM-1))/
   1(SS(2,NM)-SS(2,NM-1) )
    SS(2,NM)= ACODE
    IF (SS(2,NM-1).EQ.ACODE) SS(NN,NM) = 0.
802 CONTINUE
   0SUM(NN) = SUM(NN)+SS(NN,NM)*SIN (SS(2,NM)/57.29 )*COS(SS(2,NM)/57.
   129 )*(DTH(NM)+DTH(NM+1))/(2.0*57.29)
462 CONTINUE
   0SUM(NN)= SUM(NN)+ SS(NN,MOP)*SIN(SS(2,MOP)/57.29 )*COS(SS(2,MOP)/
   157.29 )*DTH(MOP)/(2.0*57.29 )
464 ESUM(NN) = SUM(NN)*EPASS(NN)*6.2832
    PRINT 470 ,SS(1,1),SS(2,1),SS(2,MOP),ESUM
    WRITE (2,499) SS(1,1),(ESUM(KL),KL=3,9)
470 FORMAT(F7.3,2X,2F7.2,9E10.2/)
    GO TO 480
480 DO 481 NQ= 1,25
    DO 482 NP = 1,9
482 SC(NP,NQ)= A(NP,MS+INT+NQ+1)
    PRINT 55,(SC(IZ,NQ),IZ=1,9)
    IF (NQ.EQ.1)GO TO 481
    IF (SC(2,NQ).GE.SC(2,NQ-1))483,481
483 MOB=NQ-1
    INT=INT+NQ   -1
    GO TO 490
481 CONTINUE
490 DT(MOB)= SC(2,MOB)
    MB= MOB-1
    DO 491 JO=1,MB
    DT(JO) = SC(2,JO)-SC(2,JO+1)
491 CONTINUE
    DO 494 MM=3,9
    SM(MM) = 0.0
    DO 492 NY=2,MOB
    IF (NY.EQ.MOB) GO TO 495
```

```
      IF (SC(2,NY).GT.ACODE.AND.SC(2,NY+1).GE.ACODE) SC(MM,NY)= 0.0

      IF (SC(2,NY).GE.ACODE.AND.SC(2,NY+1).LT.ACODE) 496, 495
496   SC (MM,NY) =  SC(MM,NY+1)+(SC(MM,NY)-SC(MM,NY+1))*(ACODE-SC(2,NY+1))/
     1(SC(2,NY)-SC(2,NY+1))
      SC(2,NY)= ACODE
495   SM(MM)=SM(MM)+SC(MM,NY)*SIN(SC(2,NY)/57.29)*COS(SC(2,NY)/57.29)*(D
     1T(NY)+DT(NY-1))/(2.0*57.29)
492   CONTINUE
494   ESM(MM)= SM(MM)* EPASS(MM)*6.2832
      PRINT 470, SC(1,1),SC(2,1),SC(2,MOB),ESM
      WRITE (2,499) SC(1,1),( ESM(IK),IK=3.9)
499   FORMAT(F8.3,2X,7E10.2)
      GO TO 450
      END
```